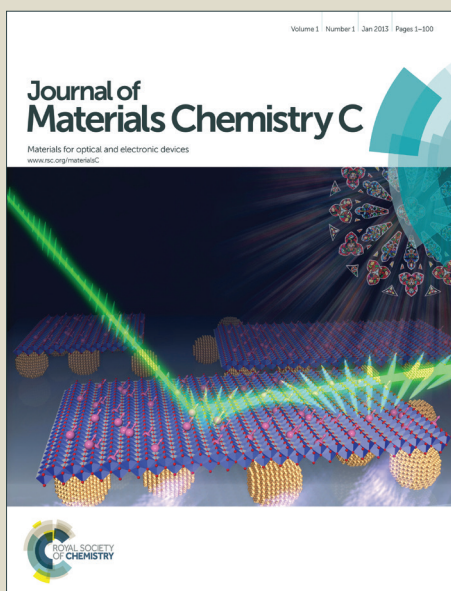


# Journal of Materials Chemistry C

Accepted Manuscript



This is an *Accepted Manuscript*, which has been through the Royal Society of Chemistry peer review process and has been accepted for publication.

*Accepted Manuscripts* are published online shortly after acceptance, before technical editing, formatting and proof reading. Using this free service, authors can make their results available to the community, in citable form, before we publish the edited article. We will replace this *Accepted Manuscript* with the edited and formatted *Advance Article* as soon as it is available.

You can find more information about *Accepted Manuscripts* in the [Information for Authors](#).

Please note that technical editing may introduce minor changes to the text and/or graphics, which may alter content. The journal's standard [Terms & Conditions](#) and the [Ethical guidelines](#) still apply. In no event shall the Royal Society of Chemistry be held responsible for any errors or omissions in this *Accepted Manuscript* or any consequences arising from the use of any information it contains.

Cite this: DOI: 10.1039/c0xx00000x

www.rsc.org/xxxxxx

ARTICLE TYPE

# Investigation of pyrolysis temperature in the one-step synthesis of L1<sub>0</sub> FePt nanoparticles from a FePt-containing metallopolymer

Qingchen Dong,<sup>\*a,b</sup> Guijun Li,<sup>c</sup> Hua Wang,<sup>a</sup> Philip Wing-Tat Pong,<sup>c</sup> Chi-Wah Leung,<sup>\*d</sup> Ian Manners,<sup>\*e</sup> Cheuk-Lam Ho,<sup>b</sup> Hua Li,<sup>b,f</sup> Wai-Yeung Wong<sup>\*a,b</sup>

Received (in XXX, XXX) Xth XXXXXXXXX 20XX, Accepted Xth XXXXXXXXX 20XX

DOI: 10.1039/b000000x

Ferromagnetic (L1<sub>0</sub> phase) FePt alloy nanoparticles (NPs) with extremely high magnetocrystalline anisotropy are considered to be very promising candidates for the next generation of ultrahigh-density data storage system. The question of how to generate L1<sub>0</sub> FePt NPs with high coercivity, controllable size, and a narrow size distribution is a challenge. We report here a single-step fabrication of L1<sub>0</sub> FePt NPs by employing one of the two new polyferroplatinyne bimetallic polymers as precursors. The influence of the pyrolysis temperature on the size and magnetic properties of the resulting FePt alloy NPs has been investigated in detail.

## Introduction

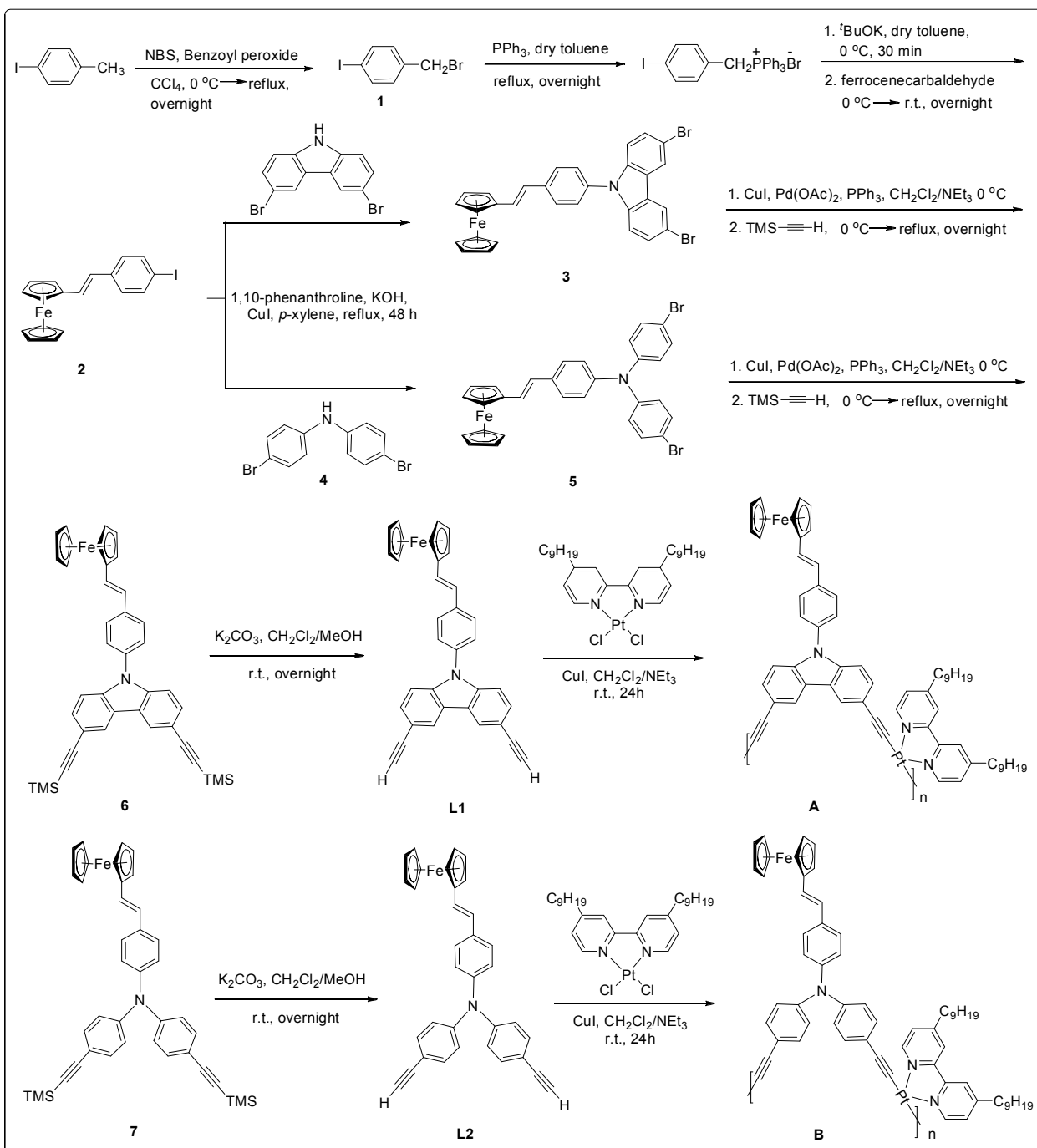
Ferromagnetic L1<sub>0</sub> phase FePt alloy nanoparticles (NPs) have attracted growing interest of researchers in the last decade, because of their interesting redox, catalytic and magnetic properties,<sup>1,2</sup> especially their potential application in next generation of ultrahigh-density magnetic data storage media, which is a consequence of its extraordinarily large uniaxial magnetocrystalline anisotropy  $K_u \approx 7 \times 10^6 \text{ J m}^{-3}$  in the bulk phase and high chemical stability.<sup>3-5</sup> FePt NPs are commonly synthesized through refluxing a Fe-source and a Pt-source together in a high boiling organic solvent. However, the superparamagnetic A<sub>1</sub> phase FePt NPs are usually formed first in this way, and a post annealing step is required to give rise to the desirable L1<sub>0</sub> phase. Inevitably, some problems such as sintering, agglomeration, broad size distribution, etc, will be concomitant with this method.<sup>6,7</sup> This might be attributed to the fact that the elements Fe and Pt reside in the separate compounds which have different onset decomposition temperatures. Hence, in this work we have prepared some organometallic complexes containing both Fe and Pt atoms and subsequently investigated their use as a single source precursor to generate the L1<sub>0</sub> phase FePt NPs by the one-step decomposition.<sup>8,9</sup> Metallopolymers have attracted intense and increasing research interest over the last two decades<sup>10-14</sup> and are of growing importance in many practical applications, e.g. photovoltaic cells,<sup>15</sup> nanocomposites,<sup>16,17</sup> biosensors,<sup>18</sup> and polymer light-emitting diodes,<sup>19,20</sup> etc. In recent years, researchers have attempted to synthesize metal NPs and metal alloy NPs by utilizing metallopolymers as templates which, on pyrolysis or photolysis, generate NPs with a narrow size distribution and a precisely controllable composition as well as density per unit area.<sup>21-27</sup> In 2008 and 2012, our groups reported a one-pot method to directly synthesize L1<sub>0</sub> FePt alloy NPs through the pyrolysis of a metallopolymer containing both Fe and Pt

atoms.<sup>28,29</sup> However, no work has been done to investigate the temperature factor of pyrolysis that controls the size and magnetic property of the resulting alloy NPs. In this work, we report the synthesis of two FePt-containing metallopolymers, followed by one-step generation of L1<sub>0</sub> FePt NPs by pyrolyzing the FePt-containing metallopolymers at different temperatures. We also investigated the effect of pyrolysis temperature on the size and magnetic properties of the resulting FePt alloy NPs.

## Results and discussion

### Synthesis and characterization of target metallopolymers

Synthesis of the target metallopolymers was performed via Sonogashira coupling reaction which gives the macromolecular products almost quantitatively. The diethynyl ligands incorporating ferrocene moiety were prepared first. Then, the coordinated Pt dichloride complex was used to couple with the diethynyl ligands to form the FePt-containing metallopolymers. Scheme 1 shows the chemical structures and the synthetic strategies to the diethynyl ligands **L1** and **L2**. To begin with, commercially available 4-iodotoluene is brominated by *N*-bromosuccinimide (NBS) and benzoyl peroxide in tetrachloromethane to give the corresponding brominated product. Then, the well-known Wittig reaction is involved in preparing the ferrocenylethylene compound. In this practical case, above 90% of the resulting product is in the *trans*-conformation. So, we separate the *trans*-product by column chromatography without further transforming little *cis*-compound into *trans*-one. The *N*-arylation of 3,6-dibromocarbazole and bis(4-bromophenyl)amine was achieved by the modified Ullmann condensation with *p*-iodoarene to result in the production of intermediates **4** and **6**, which then underwent the well-established palladium-catalyzed trimethylsilylethynylation to give trimethylsilyl-terminated compounds **7** and **8**, respectively. Finally, the TMS group was removed in the presence of potassium carbonate in methanol and



**Scheme 1.** General synthetic routes for diethynyl ligands **L1** and **L2** as well as their metallopolymers **A** and **B**

dichloromethane at room temperature to give diethynyl ligands **L1** and **L2** in up to 95% yields. Metallopolymers **A** and **B** were prepared by the CuI-catalyzed dehydrohalogenation between Pt(dipyridyl) dichloride precursor and **L1** and **L2**, respectively. Both polymers exhibit low solubility in common organic solvents.

#### 10 Pyrolysis of FePt-containing metallopolymers

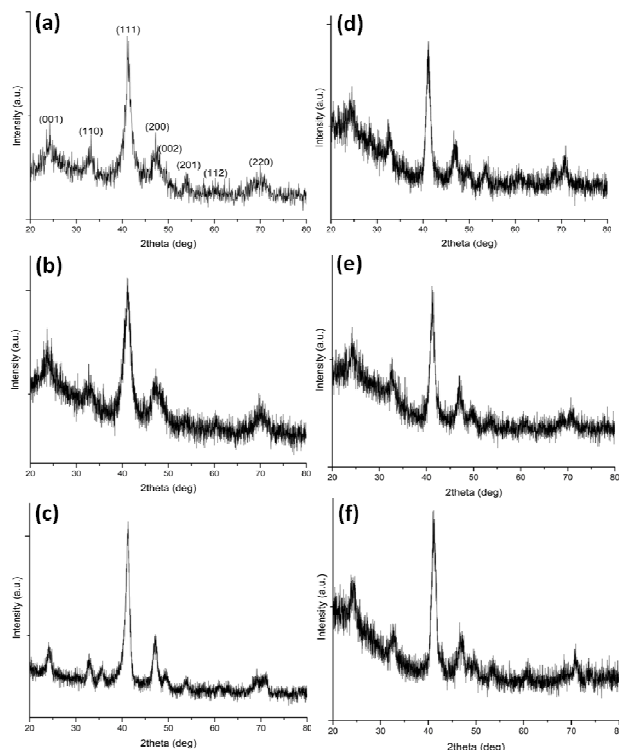
The FePt-containing metallopolymer was placed in a ceramic boat, which was then allowed to put in a tube furnace and underwent pyrolytic treatment in a nitrogen atmosphere with the heating rate of  $20^\circ\text{C min}^{-1}$  at  $600^\circ\text{C}$ ,  $700^\circ\text{C}$  and  $800^\circ\text{C}$ , respectively. Finally, the tube furnace was allowed to cool down

to ambient temperature. The NPs synthesized from pyrolysis of metallopolymer **A** at  $600^\circ\text{C}$ ,  $700^\circ\text{C}$  and  $800^\circ\text{C}$  were denoted as NP@A-600, NP@A-700 and NP@A-800, respectively, and those from pyrolysis of metallopolymer **B** were recorded as NP@B-600, NP@B-700 and NP@B-800 correspondingly.

#### Characterization of the FePt alloy NPs

Powder X-ray diffraction (PXRD) measurement was performed in order to identify the compositions and phases of the resulting NPs as-generated from pyrolysis of metallopolymers **A** and **B** at different temperatures. Fig. 1 shows the PXRD patterns of as-synthesized FePt NPs and Fig. 1(a) is the PXRD pattern of

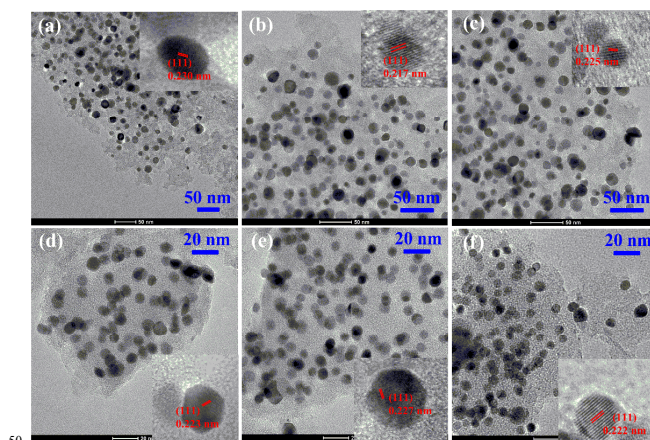
NP@A-600, in which each peak was recognized as an overall reference for other patterns. From this pattern, (001) and (110) peaks (which are the characteristic peaks for  $L1_0$  phase FePt alloy NPs<sup>30</sup>) are clearly observed at  $\sim 22^\circ$  and  $\sim 33^\circ$ . All the other samples also show the (001) and (110) peaks as well as apparent splitting of the (200)/(002) peak which signifies a tetragonality of each sample.<sup>9,30</sup> The (111) diffraction peak in each sample appears at  $2\theta = 40.96^\circ$ , which is consistent with a Fe content of



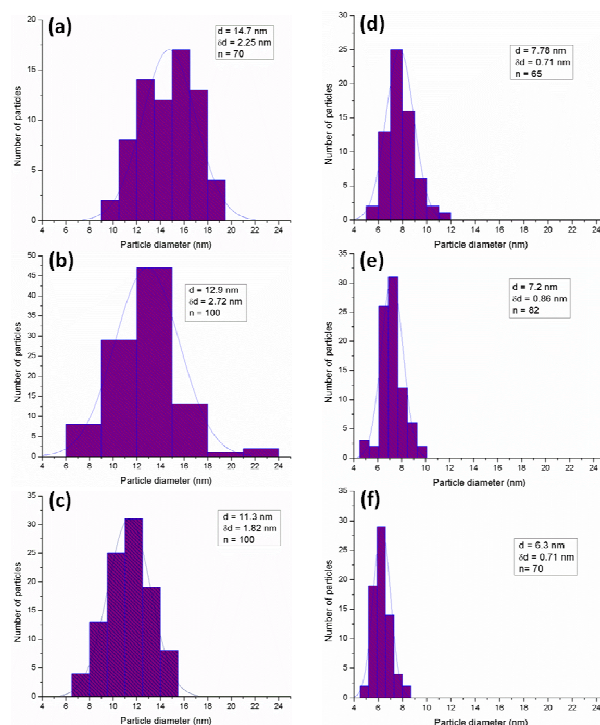
10 **Fig. 1** XRD spectra of as-prepared NPs from pyrolysis of metallopolymers A and B: (a) NP@A-600, (b) NP@A-700, (c) NP@A-800, (d) NP@B-600, (e) NP@B-700 and (f) NP@B-800.

approximately 55 atom%.<sup>30</sup> Besides, no  $Fe_xN_y$  and  $Pt_xN_y$  phases are observed in these PXRD patterns. Thus, the results of PXRD measurement suggest that the structure and composition of the resulting NPs corresponds to the pure chemically ordered  $L1_0$  FePt phase with an atomic ratio of Fe and Pt near unity. Energy-dispersive X-ray (EDX) elemental analysis for the resulting bulk FePt NPs as powder was also carried out to further verify the composition of each sample. The EDX results are tabulated in Table 1, which manifest that the ratio of Fe and Pt is approximately 50:50 as-expected for  $L1_0$  phase FePt NPs except for NP@A-800 with a slightly Pt-rich composition. This is in close agreement with the composition as inferred from the (111) peak in the PXRD pattern, and is also consistent with the stoichiometry of the metallopolymer with the near equal atomic ratio of Fe and Pt. Morphologies of the resulting FePt alloy NPs were investigated by transmission electron microscopy (TEM), as shown in Fig. 2. It can be seen clearly that all of the resulting FePt alloy NPs exhibit well-faceted spherical morphology. Insets of Fig. 2 are the high-resolution TEM images of a single FePt NP for each sample, which appeared as uncapped nanocrystals with rounded facets. The continuous fringe-patterns with interplanar distances of around 0.22 nm, corresponding to (111) d-spacing as-expected for  $L1_0$  FePt NPs, were observed conspicuously for each sample.<sup>3</sup> The well-faceted shape indicates that the NP is

highly crystalline. The NP size distribution of each sample has also been studied by analysis of the corresponding TEM images. Fig. 3 shows the histograms of the size distribution of each sample. As indicated in Fig. 3, the average NP sizes of NP@A-600, NP@A-700 and NP@A-800 are 14.7, 12.9 and 11.3 nm, respectively, with relatively broad size distribution (standard deviation ca. 15-21%). While the average NP sizes of NP@B-600, NP@B-700 and NP@B-800 are 7.78, 7.20 and 6.30 nm, respectively, and the size distribution is reasonably narrow (standard deviation ca. 9-12%). Hence, NPs generated from metallopolymer A render larger size compared to those synthesized from metallopolymer B. This could be attributed to



50 **Fig. 2** TEM and high-resolution TEM images of (a) NP@A-600, (b) NP@A-700, (c) NP@A-800, (d) NP@B-600, (e) NP@B-700 and (f) NP@B-800.



55 **Fig. 3** Particle-size histograms of as-prepared  $L1_0$  FePt NPs: (a) NP@A-600, (b) NP@A-700, (c) NP@A-800, (d) NP@B-600, (e) NP@B-700 and (f) NP@B-800.

the high onset decomposition temperature of metallopolymer B, which would result in the relatively fast nucleation of Pt followed by the diffusion of Fe into the Pt nuclei to form compact alloy NPs; also, it is noticeable that the average size of the resulting

NPs decreases with the increase of the pyrolysis temperature which is quite evident in the case of metallopolymer **B** (Fig.3). This is because chemical bonds are more rapidly cleaved at higher temperature, and thus more FePt seeds were generated, meanwhile, the organic segments originally bound to the Fe or Pt atoms would protect the FePt seeds from further sintering at higher temperature, which is similar to the function of MgO as reported by Sun *et al.* in 2009.<sup>31</sup>

**Table 1.** EDX results of NPs prepared from polymers **A** and **B**

NPs	NP@A-600		NP@A-700		NP@A-800	
	Fe	Pt	Fe	Pt	Fe	Pt
Atomic %	51	49	51	49	54	46
NPs	NP@B-600		NP@B-700		NP@B-800	
	Fe	Pt	Fe	Pt	Fe	Pt
Atomic %	50	50	49	51	49	51

#### Magnetic properties of the as-synthesized FePt alloy NPs

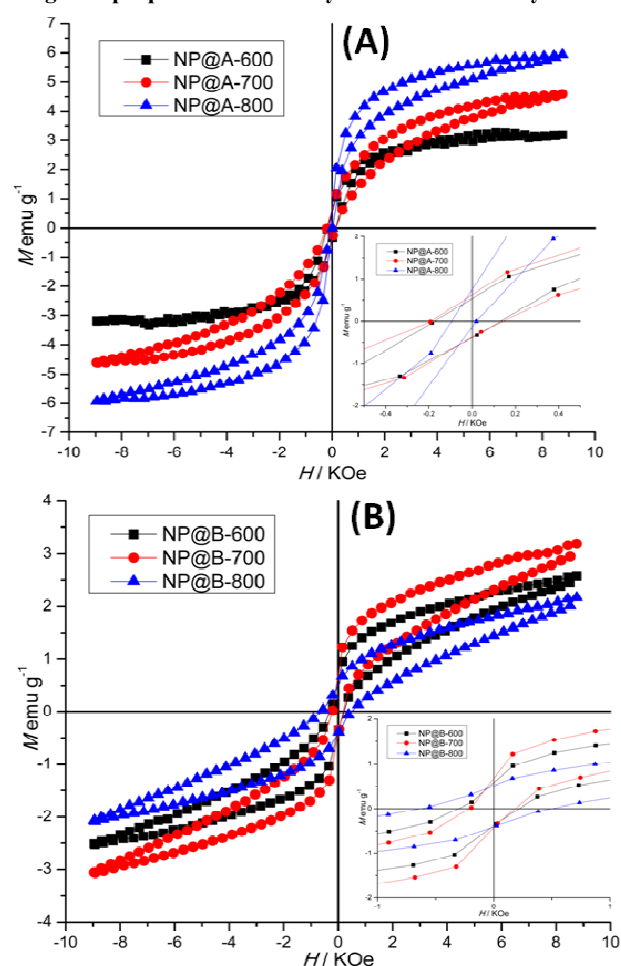


**Fig. 4** Hysteresis loops of as-prepared L1<sub>0</sub> FePt NPs measured at 300 K. The insets show the enlarged portions.

Magnetic hysteresis loops recorded for as-prepared bulk FePt NPs as powder at 300 K are shown in Fig. 4. The coercivity ( $H_c$ , an indicator of magnetocrystalline anisotropy) of NP@A-600, NP@A-700 and NP@A-800 are 175.4 Oe, 190.9 Oe, 97.1 Oe, respectively (as indicated in Fig. 4(A)). Therefore, FePt NPs pyrolyzed from metallopolymer **A** at 700 °C hold the highest  $H_c$ . While the  $H_c$  of NP@B-600, NP@B-700 and NP@B-800 are 312.9 Oe, 209.8 Oe and 622.8 Oe, respectively, demonstrating that 800 °C is the premium temperature for the generation of FePt NPs with the highest  $H_c$  using metallopolymer **B** (as indicated in Fig. 4(B)). The relationship of  $H_c$  and NP size is plotted in Fig. 5. As we can see, although there is no regular trend of  $H_c$  with the shrinkage of NP size, the FePt NPs as-prepared from metallopolymer **B** possess larger  $H_c$  in comparison to those from **A** in general. Given the size of the NPs investigated in this work, one would expect that they have single domain behavior, which normally exhibit a rising  $H_c$  with increasing particle size<sup>32</sup>; on the contrary, the opposite trend was observed in this work. However, it is noted from Fig. 3 that increasing pyrolysis temperature can give rise to *smaller* NPs. We therefore attribute the observed trend of  $H_c$  to the improved crystallinity within each NP, which is a function of pyrolysis temperature. The presence of grain boundaries within the NP can weaken the exchange coupling within the NP on one hand,<sup>33</sup> and leads to the presence of multiple anisotropy axes (and hence reduced magnetic anisotropy) on the other,<sup>34</sup> both of which causes a reduced  $H_c$ .

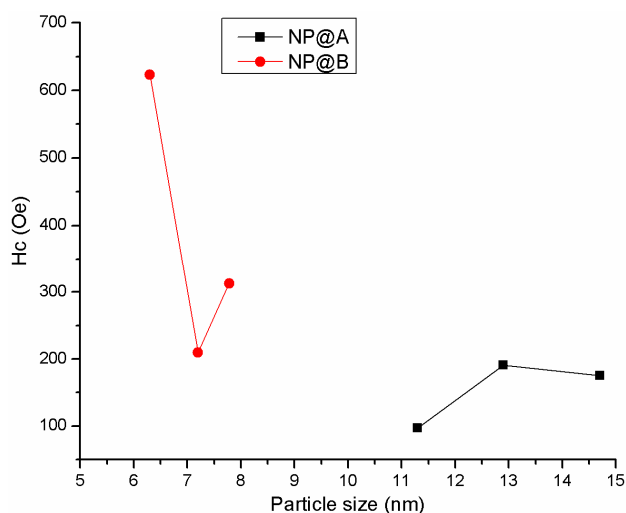


**Fig. 5** Relationship between NP size and coercivity ( $H_c$ ) of the resulting FePt NPs.

We also performed magnetic measurements at low temperature for NP@A-700 and NP@B-800 (see Fig. S1 in ESI). The results indicate that the  $H_c$  of two samples are 680 Oe (NP@A-700) and 1230 Oe (NP@B-800), respectively, which are higher than those at room temperature. More importantly, the low-temperature loops exhibit stronger contributions from the high-coercivity part of the “double coercivity” behavior. These results, together with the absence of secondary phase peaks in the XRD data, suggested that the double coercivity behavior should arise from the existence of a small amount of superparamagnetic L1<sub>0</sub> FePt NPs with ultra small size.

## Conclusions

We have presented the synthesis of two FePt-containing metallopolymer with an approximately equal atomic ratio of Fe and Pt. By taking the two metallopolymer as precursors, nearly equiatomic L1<sub>0</sub> phase FePt NPs were synthesized in a single step without any post annealing treatment as reported previously. Pyrolysis of metallopolymer **A** generated L1<sub>0</sub> FePt NPs with average size of 11.3-14.7 nm while metallopolymer **B** gave rise to L1<sub>0</sub> FePt NPs with average size of 6.3-7.78 nm. Both polymers **A** and **B** gave rise to FePt NPs with the smallest average size by pyrolyzing them at 800 °C. The TEM images indicate that the resulting FePt NPs are well-faceted spherical NPs within carbonaceous matrix which could immobilize and protect the FePt NPs. Magnetic properties of the resulting FePt NPs were investigated by VSM measurements, which manifest that NPs as-synthesized from metallopolymer **B** exhibit higher coercivity as compared to NPs generated from **A** owing to the smaller NP size. Hence, NPs as-prepared at higher temperature render smaller average size and possess larger coercivity. In the future work, we will try to purify these FePt NPs and explore their application in catalysis or biosensing.

## Experimental

### General information

All reactions were carried out under nitrogen unless otherwise stated. Commercially available reagents were used as received without further purification. All reactions were monitored by thin-layer chromatography (TLC) with Merck pre-coated glass plates. Compounds were visualized with UV light irradiation at 254 and 365 nm. Separation or purification of products was achieved by column chromatography or preparative TLC using silica gel from Merck (230–400 mesh). NMR spectra were measured in CDCl<sub>3</sub> on Bruker AV 400 NMR instrument with chemical shifts being referenced against tetramethylsilane as the internal standard for <sup>1</sup>H and <sup>13</sup>C NMR data. IR spectra were recorded on the Nicolet Magna 550 Series II FTIR spectrometer using KBr pellets for solid state spectroscopy. The positive-ion fast atom bombardment (FAB) mass spectra were recorded in *m*-nitrobenzyl alcohol matrix on a Finnigan-MAT SSQ710 mass spectrometer. Thermal analyses were performed with a Perkin-Elmer TGA 6 thermal analyzer. The molecular weight of the polymer was determined by GPC using a HP 1050 series HPLC with visible wavelength and fluorescent detectors against polystyrene standards.

### Preparation of *p*-bromomethyl iodobenzene (**1**)

To a solution of 4-iodotoluene (1.414 g, 6.48 mmol) in 15 mL of tetrachloromethane was added, with stirring and in an ice-water bath, *N*-bromosuccinimide (1.153 g, 6.48 mmol) and benzoyl peroxide (40 mg). The mixture was warmed at the reflux temperature overnight. Afterwards, the mixture was filtered and the solvent removed to give a residual solid which was purified by chromatography on a silica gel column using *n*-hexane/dichloromethane (5:1, v/v) as eluent. The *p*-bromomethyl iodobenzene was isolated as a white solid: 1.635 g (85%). <sup>1</sup>H NMR (CDCl<sub>3</sub>, 400 MHz, δ/ppm): 7.68 (d, *J* = 8.0 Hz, 2H, Ar-*H*), 7.14 (d, *J* = 8.0 Hz, 2H, Ar-*H*), 4.42 (s, 2H, ArCH<sub>2</sub>);

FAB-MS: *m/z* 413.90 (M<sup>+</sup>).

### Preparation of Preparation of 1-ferrocenyl-2-(*p*-iodophenyl)-ethene (**2**)

A solution of triphenylphosphine (177 mg, 0.67 mmol) in 20 mL of anhydrous toluene and *p*-bromomethyl iodobenzene (200 mg, 0.67 mmol) was warmed at the reflux temperature overnight to give a white solid that was filtered and washed with toluene. The *p*-iodobenzyltriphenylphosphonium bromide is a white solid: 356 mg (95%). In a three-necked round-bottom flask, previously flamed and under argon atmosphere, in an ice-water bath, was placed *p*-iodobenzyltriphenylphosphonium bromide (250 mg, 0.45 mmol) dispersed in anhydrous toluene (15 mL). To this mixture was added potassium *tert*-butoxide (76 mg, 0.675 mmol) and, after 30 min, the solution took an intense orange colour. Into this was dropped a solution of ferrocenecarbaldehyde (96 mg, 0.45 mmol) in dry toluene (5 mL). After 30 min, the mixture was stirred at room temperature overnight. Then, the solvent was removed and the residual solid was extracted with dichloromethane and purified by silica gel column chromatography using *n*-hexane/ dichloromethane (8:1, v/v) as eluent. The 1-ferrocenyl-2-(*p*-iodophenyl)-ethene was obtained as an orange solid: (298.1 mg, 72%). <sup>1</sup>H NMR (CDCl<sub>3</sub>, 400 MHz, δ/ppm): 7.63 (d, *J* = 8.0 Hz, 2H, Ar-*H*), 7.17 (d, *J* = 8.0 Hz, 2H, Ar-*H*), 6.88 (d, *J* = 16 Hz, 1H, CH=CH), 6.60 (d, *J* = 16 Hz, 1H, CH=CH), 4.46, 4.45 (s, 2H, Fc-*H*), 4.30, 4.30 (s, 2H, Fc-*H*), 4.14 (s, 5H, Fc-*H*); <sup>13</sup>C NMR (CDCl<sub>3</sub>, 125 MHz, δ/ppm): 137.64, 137.39, 128.02, 127.49, (Ar), 124.71, 91.50 (C=C), 77.21, 69.41, 69.23, 66.94 (Fc).

### Preparation of *N*-(*p*-2-ferrocenyl-ethenyl-phenyl)-3,6-dibromocarbazole (**3**)

To a solution of 1-ferrocenyl-2-(*p*-iodophenyl)-ethene (318 mg, 0.77 mmol) and 3,6-dibromocarbazole (200 g, 0.615 mmol) in 8 mL *p*-xylene, 1,10-phenanthroline (16.5 mg, 0.092 mmol) and potassium hydroxide (120 mg, 2.15 mmol) were added respectively. After the mixture was stirred at 80-100 °C for 30 min, copper iodide (17.5 mg, 0.092 mmol) and potassium hydroxide (120 mg, 2.15 mmol) were added, and the solution was allowed to reflux at 140 °C for 3 days. Then, the mixture was extracted with chloroform, and the combined organic layer was washed with water, and dried over Na<sub>2</sub>SO<sub>4</sub>. The solvent was removed and purified by silica gel column chromatography using *n*-hexane/dichloromethane (5:1, v/v) as eluent. The *N*-(*p*-2-ferrocenyl-ethenyl-phenyl)-3,6-dibromocarbazole was obtained as an orange solid (385 mg, 63%). <sup>1</sup>H NMR (CDCl<sub>3</sub>, 400 MHz, δ/ppm): 8.20 (s, 2H, Ar-*H*), 7.65 (d, *J* = 8.0 Hz, 2H, Ar-*H*), 7.51 (d, *J* = 8.0 Hz, 2H, Ar-*H*), 7.44 (d, *J* = 8.0 Hz, 2H, Ar-*H*), 7.28 (d, *J* = 8.0 Hz, 2H, Ar-*H*), 6.99 (d, *J* = 16 Hz, 1H, CH=CH), 6.78 (d, *J* = 16 Hz, 1H, CH=CH), 4.52 (s, 2H, Fc-*H*), 4.34 (s, 2H, Fc-*H*), 4.18 (s, 5H, Fc-*H*); <sup>13</sup>C NMR (CDCl<sub>3</sub>, 125 MHz, δ/ppm): 139.82, 137.81, 134.88, 129.36, 128.64, 127.14, 127.09, 124.54, 123.90, 123.19 (Ar), 113.01, 111.57 (C=C), 82.75, 69.36, 69.29, 67.05 (Fc); FAB-MS: *m/z* 611.00 (M<sup>+</sup>).

**Preparation of bis(4-bromophenyl)amine (4)**

To a stirred solution of diphenylamine (8.46 g, 50 mmol) in 50 mL of DMF at 0 °C was added dropwise a solution of *N*-bromosuccinimide (17.8 g, 100 mmol) in 50 mL DMF over 30 min. The resulting solution was allowed to stir at 0 °C for a further 6 h. Then, water was added under vigorous stirring to afford the dibrominated compound as a pure white product which was filtered off and dried *in vacuo* (16.26 g, 99%). <sup>1</sup>H NMR (CDCl<sub>3</sub>, 400 MHz, δ/ppm): 7.36 (d, *J* = 8.0 Hz, 4H, Ar-*H*), 6.92 (d, *J* = 8.0 Hz, 4H, Ar-*H*), 5.65 (s, 1H, NH); <sup>13</sup>C NMR (CDCl<sub>3</sub>, 125 MHz, δ/ppm): 141.69, 132.30, 119.48, 113.37 (Ar-C).

**Preparation of *N*-(*p*-2-ferrocenyl-ethenyl-phenyl)-3,8-dibromobiphenylamine (5)**

The procedure for the preparation of **5** was similar to that of **3**. The resulting product was obtained as a brown-yellow solid (426 mg, 57%). <sup>1</sup>H NMR (CDCl<sub>3</sub>, 400 MHz, δ/ppm): 7.36-7.31 (m, 6H, Ar-*H*), 6.99-6.94 (m, 6H, Ar-*H*), 6.79 (d, *J* = 16 Hz, 1H, CH=CH), 6.64 (d, *J* = 16 Hz, 1H, CH=CH), 4.45 (s, 2H, Fc-*H*), 4.28 (s, 2H, Fc-*H*), 4.14 (s, 5H, Fc-*H*); <sup>13</sup>C NMR (CDCl<sub>3</sub>, 125 MHz, δ/ppm): 146.34, 145.43, 133.48, 132.36, 126.82, 126.14, 125.16 (Ar), 124.61, 115.49 (C=C), 83.45, 69.22, 69.03, 66.77 (Fc).

**Preparation of *N*-(*p*-2-ferrocenyl-ethenyl-phenyl)-3,6-bis(trimethylsilylethynyl)carbazole (6)**

To an ice-cooled mixture of **3** (372 mg, 0.609 mmol) in freshly distilled triethylamine (10 mL) and CH<sub>2</sub>Cl<sub>2</sub> (10 mL) solution mixture was added CuI (20 mg), Pd(OAc)<sub>2</sub> (20 mg) and PPh<sub>3</sub> (20 mg). After the solution was stirred for 30 min at 0 °C, trimethylsilylacetylene (0.52 mL, 3.7 mmol) was then added and the suspension was stirred for 30 min in an ice-bath before being warmed to room temperature. After reacting for 30 min at room temperature, the mixture was heated to 70-80 °C for 24 h. The solution was then allowed to cool to room temperature and the solvent mixture was evaporated *in vacuo*. The crude product was purified by column chromatography on silica gel with a solvent combination of CH<sub>2</sub>Cl<sub>2</sub>/ethyl acetate (5:1, v/v) as eluent to provide *N*-(*p*-2-ferrocenyl-ethenyl-phenyl)-3,6-bis(trimethylsilylethynyl)carbazole as an orange-yellow solid (240 mg, 61%). <sup>1</sup>H NMR (CDCl<sub>3</sub>, 400 MHz, δ/ppm): 8.24 (d, *J* = 8.0 Hz, 2H, Ar-*H*), 7.63 (d, *J* = 8.0 Hz, 2H, Ar-*H*), 7.52 (d, *J* = 8.0 Hz, 2H, Ar-*H*), 7.45 (d, *J* = 8.0 Hz, 2H, Ar-*H*), 7.31 (d, *J* = 8.0 Hz, 2H, Ar-*H*), 6.98 (d, *J* = 16 Hz, 1H, CH=CH), 6.78 (d, *J* = 16 Hz, 1H, CH=CH), 4.52 (s, 2H, Fc-*H*), 4.33 (s, 2H, Fc-*H*), 4.17 (s, 5H, Fc-*H*), 0.29 (s, 18H, SiMe<sub>3</sub>); <sup>13</sup>C NMR (CDCl<sub>3</sub>, 125 MHz, δ/ppm): 140.75, 137.57, 134.77, 130.11, 128.37, 126.97, 126.93, 124.44, 122.60, 114.68 (Ar), 109.79, 105.97 (C=C), 92.25, 82.65 (C≡C), 77.08, 69.36, 69.29, 67.05 (Fc); FAB-MS: *m/z* 645.40 (M<sup>+</sup>).

**Preparation of *N*-(*p*-2-ferrocenyl-ethenyl-phenyl)-3,6-bis(trimethylsilyl-ethynyl)biphenylamine (7)**

The procedure for the preparation of **7** was similar to that of **6**. The resulting product was obtained as an orange-yellow solid (253 mg, 63%) <sup>1</sup>H NMR (CDCl<sub>3</sub>, 400 MHz, δ/ppm): 7.37-7.34 (m, 6H, Ar-*H*), 7.04-6.99 (m, 6H, Ar-*H*), 6.82 (d, *J* = 16 Hz, 1H, CH=CH), 6.67 (d, *J* = 16 Hz, 1H, CH=CH), 4.47 (s, 2H, Fc-*H*), 4.30 (s, 2H, Fc-*H*), 4.16 (s, 5H, Fc-*H*), 0.26 (s, 18H, SiMe<sub>3</sub>); <sup>13</sup>C

NMR (CDCl<sub>3</sub>, 125 MHz, δ/ppm): 147.12, 145.06, 133.78, 133.02, 126.74, 126.23, 125.26, 125.13 (Ar), 123.18, 116.99 (C=C), 105.03, 93.58 (C≡C), 83.39, 69.16, 68.97, 66.73 (Fc); FAB-MS: *m/z* 647.40 (M<sup>+</sup>).

**Preparation of *N*-(*p*-2-ferrocenyl-ethenyl-phenyl)-3,6-diethynylcarbazole (L1)**

A mixture of **6** (230 mg, 0.356 mmol) and K<sub>2</sub>CO<sub>3</sub> (111 mg, 0.803 mmol) in a mixture of methanol (8 mL) and CH<sub>2</sub>Cl<sub>2</sub> (8 mL) was stirred overnight under a nitrogen atmosphere at room temperature. The completion of the reaction was verified by spot TLC. The solvent was removed by rotary evaporation. The resulting mixture was redissolved in CH<sub>2</sub>Cl<sub>2</sub> (40 mL) and washed with three portions of 20 mL water. The light yellow organic phase was dried over anhydrous sodium sulfate and evaporated to dryness. The crude product was purified by column chromatography on silica gel eluting with hexane to provide **L1** as an orange solid (171 mg, 96%). <sup>1</sup>H NMR (CDCl<sub>3</sub>, 400 MHz, δ/ppm): 8.27 (d, *J* = 0.8 Hz, 2H, Ar-*H*), 7.65 (d, *J* = 8.0 Hz, 2H, Ar-*H*), 7.57 (d, *J* = 1.6 Hz, 2H, Ar-*H*), 7.55 (d, *J* = 1.6 Hz, 2H, Ar-*H*), 7.46 (d, *J* = 8.4 Hz, 2H, Ar-*H*), 7.00 (d, *J* = 16 Hz, 1H, CH=CH), 6.78 (d, *J* = 16 Hz, 1H, CH=CH), 4.52 (s, 2H, Fc-*H*), 4.34 (s, 2H, Fc-*H*), 4.18 (s, 5H, Fc-*H*), 3.10 (s, 2H, C≡C-*H*); <sup>13</sup>C NMR (CDCl<sub>3</sub>, 125 MHz, δ/ppm): 141.11, 137.84, 134.81, 130.45, 128.64, 127.17, 124.73, 124.60, 122.71 (Ar), 113.81, 110.16 (C=C), 84.59, 82.80 (C≡C), 75.89, 69.41, 69.35, 67.10 (Fc); FAB-MS: *m/z* 502.20 (M<sup>+</sup>); IR (KBr): 2104 (ν<sub>C=C</sub>) cm<sup>-1</sup>, 3295 (ν<sub>C≡C-H</sub>) cm<sup>-1</sup>.

**Preparation of *N*-(*p*-2-ferrocenyl-ethenyl-phenyl)-4,4-diethynyl-biphenylamine (L2)**

The procedure for the preparation of **L2** was similar to that of **L1**. The resulting product was obtained as an orange-red solid (145 mg, 98%) <sup>1</sup>H NMR (CDCl<sub>3</sub>, 400 MHz, δ/ppm): 7.36 (m, 6H, Ar-*H*), 7.03-7.01 (m, 6H, Ar-*H*), 6.81 (d, *J* = 16 Hz, 1H, CH=CH), 6.65 (d, *J* = 16 Hz, 1H, CH=CH), 4.45 (s, 2H, Fc-*H*), 4.28 (s, 2H, Fc-*H*), 4.14 (s, 5H, Fc-*H*), 3.05 (s, 2H, C≡C-*H*); <sup>13</sup>C NMR (CDCl<sub>3</sub>, 125 MHz, δ/ppm): 147.41, 145.01, 134.03, 133.21, 126.84, 126.41, 125.54, 125.10 (Ar), 123.20, 115.94 (C=C), 83.62, 83.36 (C≡C), 77.15, 69.20, 69.03, 66.78 (Fc); FAB-MS: *m/z* 503.20 (M<sup>+</sup>); IR (KBr): 2102 (ν<sub>C=C</sub>) cm<sup>-1</sup>, 3283 (ν<sub>C≡C-H</sub>) cm<sup>-1</sup>.

**Preparation of [PtCl<sub>2</sub>(<sup>109</sup>Non<sub>2</sub>bipy)]**

A suspension of K<sub>2</sub>PtCl<sub>4</sub> (100 mg, 0.245 mmol) in water was mixed with 4,4'-dinonyl-2,2'-bipyridyl (<sup>109</sup>Non<sub>2</sub>bipy, 101.6 mg, 0.245 mmol). Then, a drop of concentrated HCl was added as a catalyst. The reaction mixture was allowed to warm at 60 °C and stirred overnight. The reaction mixture was then cooled down to room temperature and extracted with dichloromethane. The crude product was purified by column chromatography on silica gel eluting with dichloromethane to provide [PtCl<sub>2</sub>(<sup>109</sup>Non<sub>2</sub>bipy)] as a bright yellow solid (140 mg, 85%). <sup>1</sup>H NMR (CDCl<sub>3</sub>, 400 MHz, δ/ppm): 9.17 (s, 2H, Ar-*H*), 7.89 (s, 2H, Ar-*H*), 7.20, 7.18 (d, *J* = 6.0 Hz, 2H, Ar-*H*), 2.81 (t, *J* = 8.0 Hz, 4H, CH<sub>2</sub>CH<sub>2</sub>), 1.76-1.72 (m, 4H, CH<sub>2</sub>CH<sub>3</sub>), 1.41-1.28 (m, 24H, CH<sub>2</sub>CH<sub>2</sub>CH<sub>2</sub>), 0.88 (t, *J* = 1.6 Hz, 6H, CH<sub>2</sub>CH<sub>3</sub>); <sup>13</sup>C NMR (CDCl<sub>3</sub>, 125 MHz, δ/ppm): 156.60, 156.39, 148.18, 126.41, 123.81 (Ar), 35.86, 32.28, 30.03,

29.95, 29.72, 27.23, 25.32, 23.05, 14.12 (C<sub>9</sub>H<sub>19</sub>).

### Synthesis and characterization of the metallopolymers

Since the metallopolymers **A** and **B** were prepared by a similar procedure, the typical method for the copper(I)-catalyzed dehydrohalogenation reaction is illustrated here by the preparation of metallopolymer **A**. To a solution of **L1** (30 mg, 0.12 mmol) in 30 ml of CH<sub>2</sub>Cl<sub>2</sub>/triethylamine (1:1, v/v) was added [PtCl<sub>2</sub>(<sup>t</sup>Non<sub>2</sub>bipy)] (81 mg, 0.12 mmol) and CuI (5 mg). The mixture was allowed to stir at room temperature for 24 h under a nitrogen atmosphere. Afterwards, the solvent was removed and the residue was redissolved in a small amount of CH<sub>2</sub>Cl<sub>2</sub> and reprecipitated from methanol. Centrifugation was performed to give **A** as a red solid (yield: 93%). Metallopolymer **B** was isolated as a red solid with a yield of 90%. For **A**: IR (KBr): 2107 (ν<sub>C=C</sub>) cm<sup>-1</sup>; GPC (THF): *M<sub>w</sub>* = 90390, *M<sub>n</sub>* = 52080, *M<sub>w</sub>*/*M<sub>n</sub>* = 1.74; Anal. calcd for C<sub>62</sub>H<sub>65</sub>N<sub>3</sub>FePt: C, 67.51; H, 5.94; N, 3.81. Found: C, 67.32; H, 6.10; N, 3.98%; *T<sub>decomp</sub>* (°C): 356 °C. For **B**: IR (KBr): 2104 (ν<sub>C=C</sub>) cm<sup>-1</sup>; GPC (THF): *M<sub>w</sub>* = 115230, *M<sub>n</sub>* = 98390, *M<sub>w</sub>*/*M<sub>n</sub>* = 1.17; Anal. calcd for C<sub>62</sub>H<sub>67</sub>N<sub>3</sub>FePt: C, 67.38; H, 6.11; N, 3.80. Found: C, 67.55; H, 6.43; N, 4.08%; *T<sub>decomp</sub>* (°C): 321 °C.

### Pyrolysis of metallopolymers

The as-synthesized metallopolymer was put in a ceramic boat, which was then placed inside a quartz reaction tube equipped with temperature and gas-flow controls. Then, the whole set-up was heated up to the desired temperature at a rate of 20 °C min<sup>-1</sup> under a nitrogen atmosphere.

### Nanoparticle characterization

Structural characterization of as-synthesized FePt NPs was performed by PXRD on a Bruker AXS D8 Advance X-Ray Diffractometer machine, with CuK<sub>α1</sub> (λ = 540 nm, 40 kV, dan 40 mA) for analyzing the composition and phase purity of the resulting NPs. TEM was performed using a Tecnai G2 20 S-TWIN for probing the morphology, particle size and size distribution of NPs. EDX spectra were obtained using a LEO 1530 scanning electron microscope for studying the ratio of Fe and Pt in the resulting metal alloy NPs. Magnetic properties of as-prepared FePt NPs were investigated at room temperature and 100 K by a Lakeshore 7407 vibrating sample magnetometer (VSM), with an applied field up to 2 T.

### Acknowledgements

We acknowledge the financial support from the National Natural Science Foundation of China (Grant No.: 61307030, 61205179, 21101111, and 51373145), Hong Kong Research Grants Council (HKBU203312), Hong Kong Baptist University (FRG2/12-13/083), Areas of Excellence Scheme, University Grants Committee of HKSAR (AoE/P-03/08) and Hundred Talents Program of Shanxi Province. The work was also supported by Partner State Key Laboratory of Environmental and Biological Analysis (SKLP-14-15-P011) and Strategic Development Fund of HKBU. Q. Dong thanks the financial support from the Program for the Outstanding Innovative Teams of Higher Learning Institutions of Shanxi (OIT), Fund Program for the

Scientific Activities of Selected Returned Overseas Professionals in Shanxi Province, the Natural Science Foundation for Young Scientists of Shanxi Province, China (Grant No.: 2014021019-2), the Outstanding Young Scholars Cultivating Program, Research Project Supported by Shanxi Scholarship Council of China (Grant No.: 2014-02) and the Qualified Personal Foundation of Taiyuan University of Technology (Grant No.: 2013Y003, tyutrc201275a). CWL acknowledges financial support from PolyU (A-PM21/G-YL07). H. Li thanks the 111 Project and Beijing Engineering Research Center of Food Environment and Public Health from Minzu University of China (No. B08044 and No.10301-01404026) for financial support. We also thank Dr. Q. Wang for assistance on the polymer synthesis.

### Notes and references

- <sup>a</sup> MOE Key Laboratory for Interface Science and Engineering in Advanced Materials and Research Center of Advanced Materials Science and Technology, Taiyuan University of Technology, 79 Yingze West Street, Taiyuan 030024, P.R. China. E-mail: dongqingchen@tyut.edu.cn.
- <sup>b</sup> Institute of Molecular Functional Materials, Department of Chemistry, Partner State Key Laboratory of Environmental and Biological Analysis and Institute of Advanced Materials, Hong Kong Baptist University, Waterloo Road, Kowloon Tong, Hong Kong, P.R. China. E-mail: rwywong@hkbu.edu.hk, Fax: +852-3411-7348
- <sup>c</sup> Department of Electrical and Electronic Engineering, The University of Hong Kong, Pokfulam Road, Hong Kong, P. R. China.
- <sup>d</sup> Department of Applied Physics, Hong Kong Polytechnic University, Hung Hom, Hong Kong, P. R. China.
- <sup>e</sup> School of Chemistry, University of Bristol, Bristol, BS8 1TS, UK. E-mail: Ian.Manners@bristol.ac.uk
- <sup>f</sup> College of Life and Environmental Sciences & Beijing Engineering Research Center of Food Environment and Public Health, Minzu University of China, Beijing 100081, P. R. China
- S. Sun, *Adv. Mater.*, 2006, **18**, 393-403.
- N. A. Frey, S. Peng, K. Cheng, and S. Sun, *Chem. Soc. Rev.*, 2009, **38**, 2532-2542.
- S. Sun, C.B. Murray, D. Weller, L. Folks and A. Moser, *Science* 2000, **27**, 1989-1992.
- (a) D. Weller and A. Moser, *IEEE Trans. Magn.*, 1999, **35**, 4423-4439 (b) J. P. Wang, *Proceedings of the IEEE*, 2008, **96**, 1847-1863.
- A. Moser, *J. Phys. D: Appl. Phys.*, 2002, **35**, R157-R167.
- T. Thomson, S. L. Lee, M. F. Toney, C. D. Dewhurst, F. Y. Ogrin, C. J. Oates and S. Sun, *Phys. Rev. B*, 2005, **72**, 064441-7.
- H. L. Nguyen, L. E. Howard, G. W. Stinton, S. R. Giblin, B. K. Tanner, I. Terry, A. K. Hughes, I. M. Ross, A. Serres and J. S. O. Evans, *Chem. Mater.*, 2006, **18**, 6414-6418.
- A. Capobianchi, M. Colapietro, D. Fiorani, S. Foglia, P. Imperatori, S. Laureti and E. Palange, *Chem. Mater.*, 2009, **21**, 2007-2009.
- M. S. Wellons, W. H. Morris, Z. Gai, J. Shen, J. Bentley, J. E. Wittig and C. M. Lukehart, *Chem. Mater.*, 2007, **19**, 2483-2488.
- V. Bellas and M. Reahn, *Angew. Chem. Int. Ed.*, 2007, **46**, 5082-5104.
- G. R. Whittell, M. D. Hager, U. S. Schubert and I. Manners, *Nat. Mater.*, 2011, **10**, 176-188.
- K. A. Williams, A. J. Boydston and C. W. Bielawski, *Chem. Soc. Rev.*, 2007, **36**, 729-744.
- B. J. Holliday and T. M. Swager, *Chem. Commun.*, 2005, **1**, 23-36.
- W. Y. Wong and C. L. Ho, *Coord. Chem. Rev.*, 2006, **250**, 2627-2690.
- W. Y. Wong, X. Z. Wang, Z. He, A. B. Djurišić, C. T. Yip, K. Y. Cheung, H. Wang, C. S. K. Mak and W. K. Chan, *Nat. Mater.*, 2007, **6**, 521-527.
- M. L. Mejía, K. Agapiou, X. Yang and B. J. Holliday, *J. Am. Chem. Soc.*, 2009, **131**, 18196-18197.
- M. L. Mejía, G. Reeske and B. J. Holliday, *Chem. Commun.*, 2010, **46**, 5355-5357.

- 18 P. Bertoncello and R. J. Forster, *Biosens. Bioelectron.*, 2009, **24**, 3191-3200.
- 19 W.-Y. Wong, *Dalton Trans.*, 2007, **40**, 4495-4510.
- 20 M. A. Rawashdeh-Omary, J. M. López-de-Luzuriaga, M. D. Rashdan, O. Elbjairami, M. Monge, M. Rodriguez-Castillo and A. Laguna, *J. Am. Chem. Soc.*, 2009, **131**, 3284-3825.
- 21 J. B. Gilroy, S. K. Patra, J. M. Mitchels, M. A. Winnik and I. Manners, *Angew. Chem. Int. Ed.*, 2011, **50**, 5851-5855.
- 22 K. Liu, S. B. Clendenning, L. Friebe, W. Y. Chan, X. Zhu, M. R. Freeman, G. C. Yang, C. M. Yip, D. Grozea, Z. H. Lu and I. Manners, *Chem. Mater.*, 2006, **18**, 2591-2601.
- 23 S. B. Clendenning, S. Aouba, M. S. Rayat, D. Grozea, J. B. Sorge, Z. H. Lu, C. M. Yip, M. R. Freeman, H. E. Ruda and I. Manners, *Adv. Mater.*, 2004, **16**, 215-219.
- 15 24 S. B. Clendenning, S. Han, N. Coombs, C. Paquet, M. S. Rayat, D. Grozea, P. M. Brodersen, R. N. S. Sodhi, C. M. Yip, Z. H. Lu and I. Manners, *Adv. Mater.*, 2004, **16**, 291-296.
- 25 J. B. Shi, C. J. W. Jim, F. Mahtab, J. Z. Liu, J. W. Y. Lam, H. H. Y. Sung, Williams, I. D.; Y. P. Dong and B. Z. Tang, *Macromolecules* 2010, **43**, 680-690.
- 20 26 J. Liu, J. W. Y. Lam, M. Häussler, A. Qin and B. Z. Tang, *J. Inorg. Organomet. Polym. Mater.*, 2009, **19**, 133-138.
- 27 W. Z. Yuan, J. Z. Sun, J. Z. Liu, Y. Dong, Z. Li, H. P. Xu, A. Qin, M. Häussler, J. K. Jin, Q. Zheng and B. Z. Tang, *J. Phys. Chem. B*, 2008, **112**, 8896-8905.
- 25 28 K. Liu, C. L. Ho, S. Aouba, Y. Q. Zhao, Z. H. Lu, S. Petrov, N. Coombs, P. Dube, H. E. Ruda, W. Y. Wong and I. Manners, *Angew. Chem. Int. Ed.*, 2008, **47**, 1255-1259.
- 29 Q. C. Dong, G. J. Li, C. L. Ho, M. Faisal, C. W. Leung, P. W. T. Pong, K. Liu, B. Z. Tang, I. Manners and W. Y. Wong, *Adv. Mater.*, 2012, **24**, 1034-1040.
- 30 30 T. J. Klemmer, N. Shukla, C. Liu, X. W. Wu, E. B. Svedberg, O. Mryasov, R. W. Chantrell, D. Weller, M. Tanase and D. E. Laughlin, *Appl. Phys. Lett.*, 2002, **81**, 2220-2222.
- 35 31 J. Kim, C. Rong, J. P. Liu and S. Sun, *Adv. Mater.*, 2009, **21**, 906-909.
- 32 C. B. Rong, D. Li, V. Nandwana, N. Poudyal, Y. Ding and Z. L. Wang, *Adv. Mater.*, 2006, **18**, 2984-2988.
- 33 G. Herzer, *IEEE Trans. Magn.*, 1989, **25**, 3327-3329.
- 40 34 W. Scholz, J. Fidler, T. Schrefl, D. Suess, H. Forster, R. Dittrich and V. Tsiantos, *J. Magn. Magn. Mater.*, 2004, **272-276**, 1524-1525.

45

### ToC Graphic

Ferromagnetic ( $L1_0$  phase) FePt alloy nanoparticles (NPs) can be generated by single-step pyrolysis of metallopolymers. The influence of the pyrolysis temperature on the size and magnetic properties of the resulting FePt alloy NPs has been investigated in detail.

